

# 1 **Surface temperature cooling trends and negative radiative forcing due to land**

## 2 **use change towards greenhouse farming in southeastern Spain**

3 Pablo Campra<sup>1</sup>, Monica Garcia<sup>2</sup>, Yolanda Canton<sup>3</sup>, Alicia Palacios-Orueta<sup>4</sup>

4 <sup>1</sup>Escuela Politécnica Superior (EPS), Universidad de Almeria, Spain

5 <sup>2</sup>Estación Experimental de Zonas Áridas (EEZA-CSIC), Almeria, Spain

6 <sup>3</sup>Departamento de Edafología y Química Agrícola, Universidad de Almeria, Spain

7 <sup>4</sup>Escuela Técnica Superior de Ingenieros de Montes. Universidad Politecnica de Madrid, Spain

8  
9 Greenhouse horticulture has experienced in recent decades a dramatic spatial expansion in  
10 the semiarid province of Almeria, in southeastern (SE) Spain, reaching a continuous area of 26,000  
11 ha in 2007, the widest greenhouse area in the world. A significant surface air temperature trend of -  
12 0.3 °C decade<sup>-1</sup> in this area during the period 1983-2006 is first time reported here. This local  
13 cooling trend shows no correlation with Spanish regional and global warming trends. Radiative  
14 forcing (RF) is widely used to assess and compare the climate change mechanisms. Surface  
15 shortwave RF (SWRF) caused through clearing of pasture land for greenhouse farming  
16 development in this area is estimated here. We present the first empirical evidences to support the  
17 working hypothesis of the development of a localized forcing created by surface albedo change to  
18 explain the differences in temperature trends among stations either inside or far from this  
19 agricultural land. SWRF was estimated from satellite-retrieved surface albedo data and calculated  
20 shortwave outgoing fluxes associated with either uses of land under typical incoming solar  
21 radiation. Outgoing fluxes were calculated from Moderate Resolution Imaging Spectroradiometer  
22 (MODIS) surface reflectance data. A difference in mean annual surface albedo of +0.09 was  
23 measured comparing greenhouses surface to a typical pasture land. Strong negative forcing  
24 associated with land use change was estimated all year round, ranging from -5.0 W m<sup>-2</sup> to -34.8 W  
25 m<sup>-2</sup>, with a mean annual value of -19.8 W m<sup>-2</sup>. According to our data of SWRF and local  
26 temperatures trends, recent development of greenhouse horticulture in this area may have masked  
27 local warming signals associated to greenhouse gases increase.

1 **Index terms:** Global change, Land cover change, Land/atmosphere interactions, Meso-scale  
2 climate change, Remote sensing

3 **Keywords:** climate change, radiative forcing, land use change, greenhouse farming, albedo,  
4 temperature trends

## 6 **1. Introduction**

7 Anthropogenic changes to the physical properties of the land surface can perturb the climate  
8 by altering the Earth's radiative energy balance, and have been regarded as a cause of regional and  
9 even global climate change [*Sagan et al.*, 1979]. Furthermore, land use changes are likely to be  
10 among the first drivers of climate change at meso- and local scales. Surface albedo affects the  
11 shortwave radiation budget by controlling how much incoming solar radiation is absorbed by the  
12 surface. Because of this, changes in surface albedo have been suspected of being the dominant  
13 influence of mid- and high- latitude land use change on climate [*Betts*, 2001]. Small changes in  
14 Earth's albedo, even below satellite detection limits, can lead to global temperature changes  
15 equivalent to those associated with increase in greenhouse gases [*Charlson et al.*, 2005].

16  
17 Radiative forcing (RF) is a useful concept to assess the relative influence of different human  
18 agents on climate change [*Forster et al.*, 2007]. The difference in outgoing shortwave (SW) fluxes  
19 between two land uses has been used as an estimation of observational SWRF due to land use  
20 change [*Betts*, 2000]. The local SWRF due to agriculture development is determined by local  
21 albedo changes, which depend on the nature of the preexisting vegetation replaced, but also on the  
22 reflectivity of the agricultural land. Employing historical reconstructions of croplands, pasture lands  
23 and primitive natural vegetation [*Ramankutty and Foley*, 1999], several estimations of global RF  
24 due to surface albedo changes from preindustrial times have been reported [*Hansen et al.*, 1998;  
25 *Betts et al.*, 2001]. These studies simulate the global shortwave radiation budget with radiative  
26 transfer models within general circulation models (GCM). In an assessment of these studies,

1 *Forster et al.* [2007] concluded a best global RF estimate of  $-0.2 \pm 0.2 \text{ W m}^{-2}$ , due to land use  
2 related surface albedo change since preindustrial times. Although the level of scientific  
3 understanding was raised by these authors to medium-low compared to very low in the previous  
4 IPCC report [*Ramaswamy et al.*, 2001], still many uncertainties rise from these estimates. On global  
5 RF estimations relative to preindustrial or preanthropogenic times, the biggest uncertainties depend  
6 on the characterization of historical and present-day vegetation and surface albedos. While there is  
7 general agreement on the albedo associated with grassland, the datasets reveal important differences  
8 between the albedo values associated with forest, shrubland and cropland [*Myhre and Myhre*,  
9 2003]. *Myhre et al.* [2005] estimated a global RF of  $-0.09 \text{ W m}^{-2}$  due to anthropogenic vegetation  
10 change since preagriculture times to present, improving the representation of current surface albedo  
11 by using data from MODIS surface albedo data.

12

13 For recent land use changes at regional or local scale these uncertainties can be overcome by  
14 observational and satellite data available. Few satellite observational estimations of RF based on  
15 anthropogenic surface albedo change at local and regional scales have been reported, and few of  
16 them quantify the impact of RF on surface temperature trends. *Fishman* [1994] reported in a field  
17 study on the meso-scale cooling effects of high albedo sandy surfaces, compared to surrounding  
18 areas. An average impact on the air temperature of 1-2°C cooler during daytime was associated to a  
19 mean difference in albedo of approximately 0.40, but no RF estimations were carried out by these  
20 authors. In another study, *Nair et al.* [2007] estimated observational RF values at the top-of-the-  
21 atmosphere (TOA) associated with clearing native vegetation for agricultural land use in southwest  
22 Australia, using observations from the Clouds and Earth's Radiant Energy System (CERES). *Jin*  
23 *and Roy* [2005] reported a positive surface RF associated with fire-induced albedo changes over  
24 half continental Australia, based on MODIS surface reflectance data. *Myhre et al.* [2005b] used  
25 Meteosat satellite data to calculate RF for changes in the surface albedo from burnt scars due to  
26 biomass burning.

1           The province of Almeria in southeastern Spain (Figure 1) has experienced from the 1970s a  
2 rapid development of greenhouse horticulture (GH). From the mid-1980s, the land covered by  
3 greenhouses doubled, reaching an area of almost 26,000 ha in 2007 [Sanjuan, 2007] (Figure 2). The  
4 coastal plain called *Campo de Dalías* accounts for 70% of total greenhouse area in the province and  
5 has become a continuous greenhouse-covered surface of 18,300 ha in 2007. Before this farming  
6 development, semiarid pasture communities had been replacing most previous natural vegetation of  
7 semiarid shrubland (*Rhamno angustifolii-Mayteneto europaei sigmetum* association) [Rivas-  
8 *Martinez*, 1985]. Favourable climatic conditions, due to high insolation (around 3,000 hours a<sup>-1</sup>) and  
9 mild temperatures during the growing season (Oct-May), with absence of frost, have been the basis  
10 for the success of greenhouse horticulture in this province, which still continues at an average net  
11 growth rate of 500 ha a<sup>-1</sup> [Sanjuan, 2007].

12  
13           Spatial patterns of temperature change for the Spanish region have been recently described  
14 using high quality controlled and homogenized series to elaborate the Spanish Daily Adjusted  
15 Temperature Series (SDATS) [Brunet *et al.*, 2006], the 22 most reliable, longest, continuous  
16 homogenized and quality-controlled surface air temperature time series in Spain. *Brunet et al.*  
17 [2007] selected these records to generate the Spanish regional temperature series (STS), composed  
18 of the regional mean, maximum and minimum temperatures time series developed from the 22 daily  
19 adjusted records. A general and highly significant warming has been observed for the 1901-2005  
20 and 1973-2005 periods, with STS annual mean temperature trends of +0.13 and +0.48 °C decade<sup>-1</sup>,  
21 respectively. Three climate stations surrounded by greenhouse development were selected in the  
22 province of Almeria as representative of GH farming area. To minimize possible impacts due to  
23 subtle circulation changes caused by agricultural land on temperature trends of nearby pasture area  
24 selected to determine SWRF, three reliable stations far enough from this area (at least 120 Km  
25 away), and with long enough available time series of temperature, were selected as temperature  
26 series controls.

1 Using an empirical approach, here we assess the hypothesis of a causal connection between  
2 SWRF associated to land use change towards greenhouse farming, and detected trends in local  
3 surface air temperature series of the last twenty years. Our assumption is that change in surface  
4 albedo due to rapid GH development has created a response in near-surface air temperature that is  
5 measurable by weather stations that monitored the farm area throughout the last decades, showing a  
6 significant cooling effect. In the null hypothesis of no differential forcing, the long-term climate  
7 trends should be very similar between greenhouse and control stations, where no localized forcing  
8 is assumed to occur.

9

10 MODIS surface albedo data were used to estimate the seasonal change in shortwave  
11 radiation budget between both land uses. To minimize differences in outgoing shortwave radiation  
12 (OSR) related to other factors than albedo change, such as spatial variability of atmospheric  
13 turbidity due to altitude, water vapor, ozone or aerosols, sectors of well conserved shrubland  
14 adjacent to greenhouse land were selected as representative of semiarid pasture surfaces for albedo  
15 and radiation measurements.

16

## 17 **2. Data and Area of Study**

18 The study area is known as *Campo de Dalías*, the widest greenhouse area in the world, and  
19 is located on the coast of the Almeria province (SE Spain) (Figure 1). It is a coastal plain with a  
20 relatively gentle relief, limited by the Mediterranean at the south and the *Sierra de Gador* range  
21 (above 2000 m high) at the north, and occupies an area of around 33,000 ha. Its climate is  
22 Mediterranean, with mild winters and low annual precipitation: average annual temperature and  
23 rainfall are 18.8 °C and 220 mm, respectively. Detailed description of the study area is provided  
24 elsewhere [*Castilla and Hernandez, 2005; Pulido-Bosch et al., 2000; Fernandez et al., 2007*]. Most  
25 greenhouses are called *parral* type, consisting of low-cost structures covered with a flat layer of  
26 plastic (polyethylene) and without heating equipment. This type of greenhouse is considered the

1 archetype of the Mediterranean greenhouse agrosystem, characterized by low technological and  
2 energy inputs [Baille, A., 2002]. During summer months, natural ventilation is not sufficient to  
3 extract excess of energy from the greenhouses, so farmers usually whiten the roofs by whitewashing  
4 (painting with slaked lime) to reduce incident radiation and avoid excess heating and humidity of  
5 growing crops inside. At the end of August, this slaked lime layer is removed to allow enough solar  
6 radiation inside for winter and spring crops.

7  
8 Long-term temperature time series (1950-2006) were obtained from meteorological stations  
9 located in Figure 1. All stations selected are outside urban locations, whether in airports or rural  
10 experimental stations, so urban heat island effects can be neglected. Two agroclimatic experimental  
11 stations in the province of Almeria were selected as GH representative sites: Mojonera (MOJ) at 36°  
12 47'N, 2° 42'W (Institute for Research and Training in Agriculture and Fisheries IFAPA, *Junta de*  
13 *Andalucia*), and Palmerillas (PAL) at 36° 48'N, 2° 43'W (*Las Palmerillas-Cajamar* Foundation  
14 Research Station). These two stations are located inside the coastal plain *Campo de Dalías*. Almeria  
15 airport station (AL) is located by the sea 20 Km east from this main greenhouse plain. Greenhouse  
16 facilities have more recently spread at the east of this station, but it is not completely surrounded by  
17 them as MOJ and PAL. Granada (GR), Malaga (MA) and Murcia (MU) airports stations, (120 km,  
18 180 km and 170 km away from AL station, respectively), were selected as control stations around  
19 the GH area, assuming negligible influence of greenhouse forcing in their climatic data. Records  
20 from GR and MA series have been recently used to elaborate the SDATS [Brunet et al., 2006]. No  
21 inhomogeneity breakpoints were found by these authors in GR and MA series for the periods  
22 considered here. GR is the only inland station and exhibits greater continentality, as it is located 600  
23 m and separated from the sea influence by Sierra Nevada (3400 m high); MA, MU, AL, MOJ and  
24 PAL stations lay next to the coast and have a milder Mediterranean climate. The stations in  
25 Southeastern Spain (MU, AL, MOJ and PAL) are characterized by a more arid climate than GR and  
26 MA. MU and AL are first order stations of the Spanish Meteorological Office (INM), and MOJ and

1 PAL are agroclimatic stations included in the cooperative network of the INM. Raw data from all  
2 stations have been subjected to different quality controls, mostly gross error checks, internal  
3 consistency, temporal and spatial coherence. Data homogenization of series not included in the  
4 SDATS was addressed based on available metadata, according to WMO Guidance on Metadata and  
5 Homogeneity [Aguilar *et al.*, 2003]. RClimDex software has been used for quality control and  
6 RHtest (with 5 years test window) was carried to detect inhomogeneities in stations at the province  
7 of Almeria. RHtest is based on a two phase regression model with a linear trend for the entire series  
8 and identifies step changes in station temperature time series [Wang, 2003]. Additionally, no  
9 statistical differences were found between MOJ and PAL time series (Kolmogorov-Smirnov test,  
10  $p>0.05$ ). Both GH stations lay just 1.8 Km from each other and are highly correlated, as shown by  
11 Pearson product-moment correlation ( $p<0.05$ ) obtained from their first difference series.

12  
13 Mean annual values for each record were obtained from monthly means based on daily  
14 maximum and minimum surface air temperatures. Records for 1950-2006 were supplied by the  
15 INM for AL, MA, MU and GR. Data from 1972 are available for these stations, but there are only  
16 common records available from 1983 for both MOJ and PAL. MOJ time series was obtained from  
17 IFAPA (Junta de Andalucia), and PAL series from *Cajamar* Foundation, and were selected as  
18 temperature series representative of the GH area (*Campo de Dalías*). Trend values are the slopes of  
19 the least-squares fit lines of mean annual temperatures versus time, in units of  $^{\circ}\text{C decade}^{-1}$ . All  
20 trends were tested for statistical significance at the 95% level.

21  
22 In order to remove the variability common to different data sets, difference time series were  
23 generated from every pair of single data series, and the significance of the trends of every difference  
24 series was then assessed. This method isolates those differences that may be attributed to  
25 differences in data set production methods, cancelling out a large fraction of the noise that obscures  
26 the underlying linear trends [Wigley *et al.*, 2006].

1 Time series of surface reflectance at 500 m resolution for the area of study were acquired  
2 from the MODIS (Moderate Resolution Imaging Spectrometer) instrument on board of the NASA  
3 Terra polar orbiting satellite for the period 2001 to 2005. The Surface Reflectance product  
4 (MOD09A1) provides surface spectral reflectance estimates for bands 1-7 corresponding to 8 days  
5 composites removing atmospheric scattering and absorption effects [Vermote and Vermeulen,  
6 1999].

7

### 8 **3. Methodology**

9 Two surface types were selected for the determination of OSR fluxes based on MODIS  
10 surface albedo data. The whole sector *Campo de Dalias* was selected as representative of  
11 greenhouse surface for OSR determination. Currently, almost 70% of this coastal plain is covered  
12 by greenhouses. The rest of the surface in this plain has been intensely anthropized and it was not  
13 possible to find parcels at MODIS resolution to represent the primitive natural vegetation or even  
14 the last pasture cover that was cleared from the 1970s for GH development. In order to represent the  
15 original pasture use of this coastal plain before the greenhouse development from the 1970s, an  
16 adjacent parcel called “Las Amoladeras” was selected (centred at 36° 49’, 2° 15’), after preliminary  
17 screening of other parcels. This is a protected and a well conserved coastal plain that lays 30 Km  
18 from the main GH area and was chosen because its current land use and vegetation are very similar  
19 to the replaced pastures of *Campo de Dalias*.

20

21 Instantaneous surface broadband albedo ( $\alpha_s$ ), representative of an 8-day period, was  
22 obtained through the equation proposed by Liang (2001):

23

$$\alpha_s = 0.160\rho_1 + 0.291\rho_2 + 0.243\rho_3 + 0.116\rho_4 + 0.112\rho_5 + 0.081\rho_7 - 0.0015 \quad (1)$$

24

1 where  $\rho$  is the reflectivity in the MODIS bands indicated by the subscript. We used the  
2 instantaneous surface albedo at the time of satellite overpass ( $\alpha_{si}$ ) as an estimate of the daily surface  
3 albedo ( $\alpha_s$ ) as *Jacob and Oliosio (2005)* demonstrated that using instantaneous values at times close  
4 to the satellite overpass in place of the daily mean albedo value did not produce significant  
5 differences ( $p < 0.01$ ). Outliers uncorrelated with the time series and with albedo values greater than  
6 0.5, corresponding to cloudy days, were identified and removed.

7  
8 In order to assess remote sensing albedo estimates, we used available field estimates of  
9 albedo obtained from the two surface types. Field measurements over the GH plastic surface were  
10 acquired on 19-06-2005, using a GER-2600 (SpectraVista) hand-held radiometer (0.35-2.51  $\mu\text{m}$ )  
11 covering 0.5  $\text{m}^2$ . Instantaneous directional albedos (nadir) were estimated at midday (12:00 h) from  
12 the ratio of outgoing/incoming radiance integral. Pasture surface albedos have been measured in  
13 Almería in a station close to our study site (Lat: 37°8'N, 2°22'W) between November and  
14 December 1997 and in spring 1998 [*Domingo et al., 2000*], using an albedometer placed 0.5 m  
15 above canopy (CM11; Kipp and Zonen, Delft, The Netherlands). Data from both types of cover  
16 were then compared with MODIS samples for the same date of spectral measurements acquisition.

17  
18 Incoming shortwave radiation at the surface (ISR) corresponding to 8 days averages was  
19 calculated daily using the solar insolation model POTRAD, which calculates the potential amount  
20 of radiation on a surface as a function of elevation, latitude and longitude, solar geometry, slope and  
21 aspect of a given site, and takes into account the influence of the surrounding topography and  
22 atmospheric transmissivity [*van Dam, 2000*]. A transmissivity value of 0.6 was used. Detailed  
23 information about clouds distribution, thickness or cloud type was not available for the study area,  
24 so clouds were not taken into account by the software. To assess the incoming shortwave radiation  
25 at surface estimated with POTRAD model, and the influence of cloud cover in the estimation, we  
26 used daily means (8-day averages) for incoming shortwave radiation ( $\text{Wm}^{-2}$ ) measured with a

1 pyranometer (CM 6B/7B Kipp & Zonen, Delft, BV), in a field experimental station located 40 km  
2 distant from the study site (Lat: 37°8'N, 2°22'W) between 2000-2005. These data were then  
3 correlated with expected insolation modeled with POTRAD for the same site and period.

4

5 The outgoing shortwave radiation OSR was estimated by equation 2 from the incoming  
6 shortwave radiation ISR and surface albedo  $\alpha$  (equation 1). Atmospheric scattering and absorption  
7 of solar radiation of reflected light at the surface were not taken into account in OSR calculations:

8

$$9 \quad \text{OSR} = \text{ISR} \times \alpha \quad (2)$$

10

11 Daily shortwave radiative forcing (SWRF) at the surface due to albedo change were  
12 calculated as the difference in the daily outgoing shortwave radiation fluxes (OSR) between the two  
13 different land use surfaces, with the formula [Betts, 2001]:

14

$$15 \quad \text{SWRF} = \text{OSR}_{\text{GREENHOUSE}} - \text{OSR}_{\text{PASTURE}} \quad (3)$$

16

17 Finally, seasonal variability curves for albedo, OSR and SWRF represent a synthetic year  
18 generated for every date from the average of the 5 records available for the period 2001-2005.

19

## 20 **4. Results**

### 21 **4.1. Surface Air Temperature Trends**

22 Remarkable warming signals have been detected for all time series available from 1972,  
23 where a clear trend change occurs after a cooling period during the 50's and 60's (Figure 3).  
24 Considering the period 1972-2006, control stations GR, MA, and MU have comparable and  
25 significant warming trends of around  $+0.5 \text{ }^\circ\text{C decade}^{-1}$  ( $p < 0.05$ ). AL trend, however, is significantly  
26 lower, with  $+0.37 \text{ }^\circ\text{C decade}^{-1}$  (Table 1). From the mid 80's, a clear divergence is shown between

1 temperatures registered at control stations and the two stations in the greenhouse area: MOJ and  
2 PAL. While control series maintain high warming trends (around  $+0.4 \text{ }^\circ\text{C decade}^{-1}$ ), MOJ and PAL  
3 show significant cooling trends ( $p < 0.01$ ) of  $-0.29 \pm 0.12$  and  $-0.32 \pm 0.11 \text{ }^\circ\text{C decade}^{-1}$ , respectively.  
4 No significant differences between these two GH time series were detected ( $p > 0.05$ ), showing  
5 similar temporal evolution. AL series shows no significant trend from 1983 ( $p > 0.1$ ), and annual  
6 mean temperatures seem to have stabilized during this period.

7  
8 Difference time series generated from every pair of single data series [Wigley *et al.*, 2006],  
9 were used to classify the pairs of stations into three time series (1983-2005) groups (Figure 4),  
10 indicating the similarities of the series in every group: control, greenhouse and AL. Very significant  
11 differences ( $p < 0.01$ ) were shown only between control (GR, MU and MA) and greenhouse stations  
12 (MOJ/PAL). AL showed again an intermediate behaviour, with lower but significant trend  
13 differences when paired with either control or greenhouse stations. Trend differences were not  
14 significant among control stations difference series ( $p > 0.8$ ), and between MOJ and PAL ( $p > 0.5$ ),  
15 indicating the high degree of homogeneity of their time series.

#### 16 17 **4.2. Seasonal Variations in Surface Albedo**

18 Surface albedo values of greenhouse surface were consistently higher than pasture values in  
19 all seasons, with annual average values of  $0.28 \pm 0.05$  and  $0.19 \pm 0.02$ , respectively (Figure 5).  
20 Albedo values exhibited strong seasonality, with a maximum value for GH of 0.35 measured in  
21 summer, and a minimum of 0.20 in winter. Pasture surface albedo showed lower seasonal variation,  
22 from 0.22 in summer to 0.16 in winter. Biggest differences in albedo between GH and pasture  
23 surfaces of approximately 0.15 were measured in summer, and the smallest difference of 0.05  
24 registered in winter, with a mean annual value of 0.09. It is noticeable the asymmetric shape of GH  
25 and difference curves, with a step decrease from maximum summer values and a gradual increase  
26 from winter minimum value, not reflected in the pasture curve.

1

2 A mean daily albedo value of  $0.4 \pm 0.06$  was obtained in the field over plastic GH cover with  
3 the spectroradiometer at the available date. In order to compare with MODIS daily albedo estimate,  
4 we have to take into account that MODIS GH pixels ( $1 \text{ km}^2$ ) include minor portions of other types  
5 of land use (bare soil, roads, etc) with lower reflectivity than plastic surface. Nonetheless, when  
6 MODIS GH pixels ( $n=45$ ) with the highest proportion of greenhouses cover were selected, albedo  
7 estimated for the same date was  $0.36 \pm 0.04$ . For pasture land the albedometer provided an average  
8 daily albedo value of  $0.158 \pm 0.002$ , for available dates [Domingo *et al.*, 2000], comparable to  
9 MODIS pasture estimates for the same period.

10

### 11 **4.3. Seasonal Variations in Outgoing Shortwave and SW Radiative Forcing (SWRF)**

12 Annual mean incoming SW radiation at greenhouse surface was  $195.98 \text{ W m}^{-2}$  for the 2001-  
13 2005 period, with values ranging from  $86.97 \text{ W m}^{-2}$  in winter to  $298.11 \text{ W m}^{-2}$  (data not shown).  
14 Seasonal variations of diurnally averaged OSR for greenhouse and pasture areas, as well as the  
15 difference time series for the period of study are represented in Figure 6. Strong differences  
16 between both land use types were observed, with higher values over greenhouse areas all year  
17 around due to higher albedo of plastic cover. Mean OSR annual values were  $58.4 \text{ W m}^{-2}$  for GH and  
18  $38.5 \text{ W m}^{-2}$  for pasture. Maximum fluxes were detected in summer for both surfaces, with  $98 \text{ W m}^{-2}$   
19 and  $65 \text{ W m}^{-2}$  for GH and pasture, respectively. OSR showed the lowest values in winter, with 20  
20  $\text{W m}^{-2}$  for GH and  $13 \text{ W m}^{-2}$  for pasture. The range of seasonal variation is much wider in GH ( $78$   
21  $\text{W m}^{-2}$ ) than in pasture ( $51 \text{ W m}^{-2}$ ).

22

23 In Figure 6 observational SWRF due to land use change is represented by the difference  
24 between GH and pasture OSR averaged values for the 2000-2005 period (plotted here with opposite  
25 sign to RF). Mean annual SWRF was  $-19.8 \text{ W m}^{-2}$ . Minimum forcing remained almost constant  
26 (between  $-5$  and  $-6 \text{ W m}^{-2}$ ) during November and December, gradually increasing since January to a

1 maximum value by the end of July of  $-34.8 \text{ W m}^{-2}$ . From August, a steep decrease in the forcing is  
2 observed, falling by the end of October next to the minimum annual values. This asymmetry in the  
3 seasonal difference curve is determined by the asymmetric shape of both the albedo and OSR  
4 curves for GH surface (Figures 5 and 6). This curve shape is not depicted by the more symmetric  
5 pasture albedo and OSR curves.

## 7 **5. Discussion**

### 8 **5.1. Surface Air Temperature Trends**

9 Mean annual temperature trends for control time series GR, MA and MU agree with  
10 northern hemisphere reported warming trends for the last three decades [*Trenberth et al.*, 2007;  
11 *Brohan et al.*, 2006], as well as with regional trends for Spain (STS) and Europe [*Klein Tank et al.*,  
12 2002; *Castro et al.*, 2005; *Brunet et al.*, 2007]. Temperature fluctuations shown in the time series  
13 (Figure 3) are attributed to natural processes (such as major volcanic eruptions, ENSO, QBO, etc.),  
14 and mean short breakpoints in the long term warming were detected in all control stations. The most  
15 remarkable in all series is the sudden cooling following the eruption of Mt. Pinatubo in 1991.  
16 Nevertheless, trend differences between controls and stations in Almeria province (MOJ/PAL/AL)  
17 are consistent with our hypothesis that a massive growth of greenhouse horticulture has impacted  
18 long-term trends in surface temperatures of these farming areas. AL station is adjacent to high  
19 albedo surfaces, and shows a weaker forcing effect than GH stations completely surrounded by  
20 agricultural land (MOJ and PAL). The three temperature series in the province of Almería also  
21 clearly disagree with the pattern of variability for southeastern and eastern Spain from 1973 to 2005  
22 reported by *Brunet et al.*, [2007], with an annual trend of  $+0.54 \text{ °C decade}^{-1}$  that indicates a strong  
23 rise in temperatures and accelerated warming over this subregion.

### 25 **5.2. Seasonal Variations in Surface Albedo**

1 Mean surface albedo value measured for GH (0.28) is higher than previous estimates of  
2 cropland albedo at global scale, ranging from 0.15 to 0.20 [Myhre and Myhre, 2003]. Nevertheless,  
3 our estimation was calculated for the whole coastal plain of *Campo de Dalias*, and there is a wide  
4 range of variation depending on the parcel selected (data not shown). Most important variability in  
5 GH albedo depend on whether annual whitewashing of the plastic surface had been applied or not.  
6 Smaller GH parcels screened (data not shown) where whitewashing had been fully applied, showed  
7 the maximum mean annual albedo values of  $0.32 \pm 0.03$ , but were not considered representative of  
8 the whole GH area selected (*Campo de Dalias*), that includes small fractions of other types of land  
9 uses apart from greenhouses, such as urban cover or abandoned farmland.

10  
11 The observed asymmetry in the shapes of GH albedo and OSR curves (Figure 6) is probably  
12 attributable to the annual timing of the whitewashing of the plastic covers carried out regularly by  
13 farmers. Whitewashing is performed during summer to prevent summer crops from damage caused  
14 by insolation excess. After summer, the slaked-lime is washed out to get adequate radiation  
15 conditions during the last stage of winter crops (January-February) and the crops change.

16  
17 Mean annual surface albedo of the pasture area selected (0.19) was inside the range of  
18 values for shrubland previously reported at global scale (0.16-0.29) [Myhre and Myhre, 2003]. In  
19 preliminary estimations of surface albedo of other pasture parcels screened nearby the GH area, a  
20 range of 0.13 to 0.19 was measured depending on surface reflectance, but we selected our  
21 representative parcel of study according to higher similarities with past pastures cleared for GH  
22 development in the coastal plain. Clearing of pasture land for GH development follows the  
23 maximum pattern previously reported for the increase in the surface albedo in the Northern  
24 Hemisphere midlatitudes, considering anthropogenic vegetation changes from preagriculture times  
25 to present [Myhre and Myhre, 2003], particularly evident in eastern Europe and the eastern United  
26 States caused by the conversion of forest to cropland. In our area of study, the measured increase of

1 the annual mean surface albedo of +0.09 is similar to the maximum values calculated at global scale  
2 (around +0.10) [Betts, 2001]. Therefore, extensive white plastic cover has a comparable effect on  
3 the differences in mean annual albedo as long-lasting snow cover at high latitudes exerts related to  
4 previous forest coverage. On the contrary, this increase in GH albedo is opposite to the decrease in  
5 the farmland surface albedo of approximately between -0.02 and -0.01 simulated for Mediterranean  
6 latitudes in those studies, related to preagriculture times.

7

### 8 **5.3. Seasonal Variations in Outgoing Shortwave and SW Radiative Forcing (SWRF)**

9 The magnitude of localized SWRF due to GH development over the last decades reported  
10 here ( $-19.8 \text{ W m}^{-2}$ ) is considerably greater than most previous computations of simulated global  
11 mean RF due to land use change over the past [Hansen *et al.*, 1998; Betts, 2000, 2001; Myhre *et al.*,  
12 2005a]. Although it has been considered  $-0.2 \text{ W m}^{-2}$  a good estimation for this global forcing since  
13 preindustrial times [Forster *et al.*, 2007], most of these global simulations show a very high degree  
14 of spatial variability, with regions showing the strongest local negative RF ( $-5 \text{ W m}^{-2}$ ) found in the  
15 major agricultural areas of North America and Eurasia. In some of these estimations, the increase in  
16 surface albedo due to long-lasting winter snow cover in northern deforested latitudes is again  
17 responsible for the maximum negative RF estimated values ( $-10 \text{ W m}^{-2}$ ) [Myhre *et al.*, 2005a].  
18 Mean annual SWRF due to GH development ( $-19.8 \text{ W m}^{-2}$ ) almost doubles the magnitude of this  
19 global maximum, thus reflecting the relative strength of the localized forcing over the last decades  
20 in the area of study. Furthermore, GH albedo change maximize in the period with maximum solar  
21 radiation (Figure 5) while deforestation at northern latitudes has a maximum albedo change when  
22 solar radiation has its minimum [Myhre, *pers. comm.*, 2008].

23

24 Our observational estimation largely offsets the positive forcing of approximately between  
25  $+2$  and  $+6 \text{ W m}^{-2}$  assigned to this region in global simulation studies from preagriculture times, and  
26 of course, the global forcing relative to preindustrial times exerted by greenhouse gases, estimated

1 at  $+2.3 \text{ W m}^{-2}$  [Hansen *et al.*, 1998]. In one of the few related studies on observational estimation of  
2 forcing associated with land use change at regional scale to date [Nair *et al.*, 2007] an observational  
3 estimate of mean annual SWRF of  $-7.0 \text{ W m}^{-2}$  was reported in Southwest Australia, due to land use  
4 change for agricultural purposes, considering that half of the whole area of study had been cleared.  
5 These authors estimated a maximum SWRF value of  $-13.9 \text{ W m}^{-2}$  in case 100% of the land was  
6 cleared. Though our SWRF estimate refers to a 70% GH cover, alternative forcing measurements in  
7 minor parcels with an almost complete coverage of GH reached the strongest SWRF of  $-30.2 \text{ W m}^{-2}$   
8 (data not shown).

9  
10 As stated before [Myhre and Myhre, 2003], the most important source of uncertainty in the  
11 estimation of RF due to land use change is the correct characterization of surface albedo, that  
12 depends on both the pasture vegetation and soil, and the reflectance of the plastic surfaces to be  
13 compared. In this case, the selection of the parcels representative of preexisting pasture land cover  
14 cleared for GH development and the variation in albedo due to the heterogeneity of whitewash  
15 surface can extent the range of mean annual SWRF from  $-19 \text{ W m}^{-2}$  to a maximum of  $-37 \text{ W m}^{-2}$   
16 (data not shown). The degree of vegetation cover of the pastures studied for SWRF estimation,  
17 varying from shrubland to grassland, is in great part responsible for this variability. Nevertheless,  
18 we considered GH and pasture parcels selected as the most representative of both land uses,  
19 although they yielded the weaker negative SWRF of all pairs of parcels compared in preliminary  
20 screening.

21  
22 Another source of uncertainty is the temporal variability of incoming SW radiation observed  
23 with instrumental data due to cloudiness or changes in atmospheric conditions. This temporal  
24 variability, as represented by the average of standard error for each date during the recorded period,  
25 represents a small percentage of the mean annual incoming shortwave radiation at this region (4.75  
26 %). High correlation was found between field measures and POTRAD modelled insolation series

1 for clear sky conditions (Pearson-correlation coefficient = 0.97; Root Mean Square Error = 16.93  
2  $\text{Wm}^{-2}$ ; Mean Annual Error = 3%, expressed as a percentage of the mean of n=46 dates). Therefore,  
3 it can be assumed that the level of uncertainty due to cloudiness in SWRF estimates using the  
4 POTRAD model is low.

5  
6 While there could be a strong correlation between the decrease in temperature records and  
7 the increase in SWRF due to GH development, this does not necessarily imply that albedo change is  
8 the main causative factor of the observed trends, as reflectivity alterations are not the only effect of  
9 land use change on climate. Local climate sensitivity to GH forcing needs further studies to be  
10 determined. Related cooling effects of historical land use change towards higher-albedo surfaces  
11 have been simulated [*Brovkin et al.*, 1999; *Betts*, 2001], suggesting that albedo difference is the  
12 main driver of temperature change in temperate agricultural regions. Although global mean climate  
13 response can be small due to a weak global albedo forcing, the response can be remarkable in some  
14 regions, as can be seen when spatial distribution of this forcing is considered [*Hansen et al.*, 2005].  
15 Through these models, annual mean temperatures 1-2 K lower than natural vegetation have been  
16 simulated for some agricultural regions, in response to increases in surface albedo of +0.1,  
17 comparable to GH development increase reported here. In those cases, the main vegetation change  
18 was the conversion of forest to cropland in high latitudes, where snow-covered areas have much  
19 higher surface albedo over open land (as cropland) than in forested areas.

20  
21 Previous observational studies show a dominant influence of high albedo surfaces on local  
22 surface temperature trends [*Fishman et al.*, 1994]. *Christy et al.* [2006] have reported the darkening  
23 and moistening of formerly dry high-albedo surface in semiarid environments as the main cause of  
24 increase in surface temperatures caused by farming development in California San Joaquin Valley.  
25 In our case, however, the change is an increase in surface albedo, and though the influence of  
26 irrigation under a plastic surface still remains undetermined, cooling temperature trends indicate

1 that it probably has little impact compared to negative forcing exerted by increased surface  
2 reflectivity.

3

#### 4 **6. Conclusions**

5 Our results show that, at local and meso-scale, greenhouse farming is very likely the most  
6 powerful driver of climate change in the area of study, probably due to the dramatic increase in  
7 surface albedo of the highly reflective plastic cover over a widespread agricultural area, which  
8 largely offsets positive forcing ( $+2 \text{ W m}^{-2}$ ) very probably induced by global increase in greenhouse  
9 gases [Forster *et al.*, 2007]. The main general implication of these findings is to highlight the  
10 importance of human development of high albedo surfaces in the strategies of mitigation and  
11 adaptation to global warming at local scale. However control stations records outside the GH area  
12 show that little or no effects on surface temperature extend far from the high albedo area, so the  
13 forcing caused by greenhouse development seems to be very localized.

14

15 Although other climate change agents out of the scope of this work cannot be ruled out, the  
16 attribution of the temperature cooling trend in GH area to a negative radiative forcing due to change  
17 in surface albedo is strongly supported by our analyses of satellite data. The most likely explanation  
18 is that higher surface albedo reduces net incoming shortwave energy, and therefore diminishes the  
19 energy absorbed by the surface emitted as longwave radiation, resulting in lower surface skin  
20 temperature, as well as a lower transfer of sensible heat over greenhouses with respect to pasture  
21 cover. The lower surface temperature, and the decrease in the total available energy at the surface  
22 that needs to be dissipated, generates the cooling trend detected in the near-surface air temperatures  
23 in this farming area

24

25 Further analyses must be undertaken to establish or refute causality between SWRF and  
26 temperature trends discussed here. The purpose of this work is to present the first empirical

1 evidences of this causal connection through an estimation of SW budget inside and outside the GH  
2 area, but other significant feedbacks to the atmosphere from changes in the cover of terrestrial  
3 surface by greenhouse farming still remain to be investigated. Model-simulations and radiative  
4 transfer calculations including constraints arising from high albedo GH surfaces at the temporal and  
5 spatial scale of this study should be carried out in order to corroborate our results by comparison of  
6 expected responses to detected temperature trends. However, evaluation of net radiation and soil  
7 heat transfer at daily scales, and quantification of the turbulent fluxes (sensible and latent heat), are  
8 necessary to fully determine how the surface energy balance is affected by the changes in cover:

9

- 10 - Uncertainties in the local energy budget must be reduced with the determination of longwave  
11 fluxes, and net radiative forcing due to short plus longwave differences between both land uses  
12 has yet to be quantified. Nevertheless, it is important to notice that when comparing RF values  
13 from earlier estimates, it has been assumed in this work that net forcing is dominated by the  
14 shortwave component and that land use changes do not significantly impact the TOA longwave  
15 fluxes [*Nair et al.*, 2007].
- 16 - The relative influence on local climate of other physical changes must be explored. The land use  
17 climate forcing that we have estimated here does not fully represent GH land use effects, as  
18 there are other changes in surface properties affecting the surface energy balance that have not  
19 been considered. For instance, eco-physiological and aerodynamic changes and alterations of  
20 roughness still remain undertermined. The complex role of evapotranspiration associated to this  
21 drip-irrigated soil under a plastic cover must be investigated [*Fernandez et al.*, 2007]. Cooling  
22 effect of higher albedo could have been enhanced by the increase in latent heat flux derived  
23 from irrigation within the greenhouses (released as water vapor by greenhouses ventilation),  
24 with respect to previous pasture cover, further reducing sensible heat transfer and surface air  
25 temperature. On the contrary, irrigation might also cause a positive forcing by the increase in  
26 water vapor in the lower atmosphere [*Boucher et al.*, 2004; *Christy and Norris*, 2006].

- 1 - In order to assess the net influence of greenhouse farming on local climate, the role of annual  
2 biomass growth as carbon sink must be quantified and expressed as RF [Betts, 2000]. While  
3 forestation at northern latitudes and most conventional crops are generally associated to positive  
4 forcing by reduction in surface albedo, greenhouse development in semi-desert surfaces exert a  
5 negative forcing that is probably further increased by the forcing caused by carbon sequestration  
6 of these highly productive crops.
- 7 - Even the RF concept might not be the most appropriate concept in our case, so that other  
8 alternative metrics [Pielke et al., 2002] could be advisable to estimate and modelize the net  
9 impact on the local climate of GH development.

10

11 **Acknowledgements.** We thank the INM (Spanish National Institute of Meteorology), Cajamar  
12 Foundation and IFAPA (Junta de Andalucia) for providing climatic data.

13

#### 14 **References**

15 Aguilar, E., I. Auer, M. Brunet, T.C. Peterson, and J. Wieringa (2003), Guidelines on climate  
16 metadata and homogenization. WCDMP-No. 53, WMO-TD No. 1186. World Meteorological  
17 Organization: Geneva.

18

19 Albert, K.T., J. Wijngaard and A. Engelen (2002), Climate of Europe; Assessment of observed  
20 daily temperature and precipitation extremes, KNMI, De Bilt, The Netherlands, 36pp.

21

22 Baille, A. (2002), Trends in greenhouse technology for improved climate control in mild winter  
23 climates, *Acta Hort*, 559, 161-167.

24 Betts, R.A. (2000), Offset of the potential carbon sink from boreal forestation by decreases in  
25 surface albedo, *Nature*, 408, 187-190.

- 1 Betts, R. A. (2001), Biogeophysical impacts of land use on present-day climate: near-surface  
2 temperature change and radiative forcing, *Atmospheric Sci. Lett.*, doi:1006/asle.2001.0023.
- 3 Boucher, O., G. Myhre and A. Myhre (2004), Direct human influence of irrigation on atmospheric  
4 water vapour and climate, *Clim. Dyn.*, 22, 597-603.
- 5 Brohan, P., J.J. Kennedy, I. Haris, S.B.F. Tett and Jones, P.D. (2006), Uncertainty estimates in  
6 regional and global observed temperature changes: A new dataset from 1850, *J. Geophys. Res.*,  
7 11, D12106, doi:10.1029/2005JD006548.
- 8 Brovkin, V., A. Ganapolski, M. Claussen, C. Kubatzki, and V. Petoukhov (1999), Modelling  
9 climate response to historical land cover change. *Global Ecol. Biog.*, 8, 509-517.
- 10
- 11 Brunet, M., O. Saladie, P.D. Jones, J. Sigro, A. Moberg, E. Aguilar, A. Walther, D. Lister, D.  
12 Lopez, and C. Almarza (2006), The development of a new daily adjusted temperature dataset for  
13 Spain (1850-2003), *International Journal of Climatology* 26: 1777-1802.
- 14
- 15 Brunet, M., O. Saladie, P.D. Jones, J. Sigro, A. Moberg, E. Aguilar, A. Walther, Della-Marta, P., D.  
16 Lister, Walther, A., D. Lopez and C. Almarza (2007), Temporal and spatial temperature  
17 variability and change over Spain during 1850-2005. *J. Geophys. Res.-Atmosphere*, 112, DOI:  
18 10.1029/2006JD008249.
- 19
- 20 Castilla N. and J. Hernandez (2005), The plastic greenhouse industry in Spain, *Chronica Hort.* 45,  
21 15-20.
- 22
- 23 Castro, M., J. Martín-Vide and S. Alonso (2005), El clima de España: pasado, presente y escenarios  
24 del clima para el siglo XXI, in: *Evaluación Preliminar de los Impactos en España por Efecto del*  
25 *Cambio Climático* [Moreno, J.M. (Coord.)], Ministerio de Medio Ambiente, Madrid, Spain.

- 1
- 2 Charlson R.J., F.P.J. Valero and J.H. Seinfeld (2005), In Search of Balance, *Science*, 308, 806-807.
- 3
- 4 Christy, J.R., W.B. Norris, K. Redmon and K.P. Gallo (2006), Methodology and Results of  
5 Calculating Central California Surface Temperature Trends: Evidence of Human-Induced Climate  
6 Change, *J. Climate*, 19, 548-563.
- 7
- 8 Domingo, F., Villagarcía, L., Brenner, A.J., Puigdefabregas J. (2000), Measuring and modelling the  
9 radiation balance of a heterogeneous shrubland, *Plant, Cell & Environment* 23, 27-38.  
10 doi:10.1046/j.1365-3040
- 11
- 12 Fernandez, M.D., A.M. Gonzalez, J. Carreño, C. Perez and S. Bonachela (2007), Analysis of on-  
13 farm irrigation performance in Mediterranean greenhouses, *Agricultural Water management*, 89,  
14 251-260.
- 15 Fishman, B., H. Taha, and H. Akbari (1994), *Mesoscale Cooling Effects of High-Albedo Surfaces:  
16 Analysis of Meteorological Data from White Sands National Monument and White Sands Missile  
17 Range*, Lawrence Berkeley Laboratory report No. 35056.
- 18 Forster, P. et al. (2007), Changes in Atmospheric Constituents and in Radiative Forcing, in: *Climate  
19 Change 2007: The Physical Science Basis. Contribution of Working Group I to the Fourth  
20 Assessment Report of the Intergovernmental Panel on Climate Change* [Solomon, S., D. Qin, M.  
21 Manning, Z. Chen, M. Marquis, K.B. Averyt, M.Tignor and H.L. Miller (eds.)]. Cambridge Univ.  
22 Press, Cambridge, United Kingdom and New York, NY, USA.
- 23 Hansen, J., M. Sato, A. Lacis, R. Ruedy, I. Tegen, and E. Matthews (1998), Climate forcings in the  
24 Industrial Era, *Proc. Natl. Acad. Sci. U. S. A.*, 95, 12,753– 12,758.

- 1 Hansen, J., et al. (2005), Efficacy of climate forcings, *J. Geophys. Res.*, *110*, D18104,  
2 doi:10.1029/2005JD005776.
- 3 Jacob, F. and A. Oliosio (2005), Derivation of diurnal courses of albedo and reflected solar  
4 irradiance from airborne POLDER data acquired near solar noon *J. Geoph. Res. Atm.*, *110 (D10)*:  
5 D10104.
- 6 Jin, Y. and D.P. Roy (2005), Fire-induced albedo change and its radiative forcing at the surface in  
7 northern Australia, *Geophys. Res. Lett.*, *32*, L13401 doi:10.1029/2005GL022822
- 8 Kiehl, J. T. and K.E. Trenberth (1997), Earth's Annual Global Mean Energy Budget, *Bull. Amer.*  
9 *Meteor. Soc.*, *78*, 197-208.
- 10 Liang, S. L. (2001), Narrowband to Broadband Conversions of Land Surface Albedo I Algorithms.  
11 *Remote Sens. Environ.*, *76*, 213-238.
- 12 Myhre, G. and Myhre, A. (2003), Uncertainties in Radiative Forcing due to Surface Albedo  
13 Changes Caused by Land-Use Changes, *J. Climate*, *16*, 1511-1524.
- 14 Myhre, G., Kvaleva M.M. and Schaaf C.B (2005a), Radiative forcing due to anthropogenic  
15 vegetation change based on MODIS surface albedo data, *Geophys. Res. Lett.* *32*, L21410,  
16 doi:10.1029/2005GL024004.
- 17 Myhre, G., Y. Govaerts, J. M. Haywood, T. K. Berntsen, and A. Lattanzio (2005b), Radiative effect  
18 of surface albedo change from biomass burning, *Geophys. Res. Lett.*, *32*, L20812,  
19 doi:10.1029/2005GL022897.
- 20 Nair, U. S., D.K Ray., J. Wang, S.A. Christopher, T.J. Lyons, R.M. Welch and R.A. Pielke (2007),  
21 Observational estimates of radiative forcing due to land use change in southwest Australia. *J.*  
22 *Geophys. Res.*, *112*, D09117, doi:10.1029/2006JD007505.

- 1 Pielke, R.A., G. Marland, R.A. Betts, T.N. Chase, J.L. Eastman, J.O. Niles, D. Niyogi and S.W.  
2 Running (2002), The influence of land-use change and landscape dynamics on the climate system:  
3 relevance to climate-change policy beyond the radiative effect of greenhouse gases, *Phil. Trans.*  
4 *R. Soc. Lond.*, 360, 1–15.
- 5 Pulido-Bosch, A., P. Pulido-Leboeuf, L. Molina-Sanchez, A. Vallejos, W. Martin-Rosales (2000),  
6 Intensive agriculture, wetlands, quarries and water management. A case study (*Campo de Dalías*,  
7 SE Spain). *Environmental Geology*, 40, 163-168.
- 8 Ramankutty, N., and J. A. Foley (1999), Estimating historical changes in global land cover:  
9 Croplands from 1700 to 1992, *Global Biogeochem. Cycles*, 13, 997– 1027.
- 10 Ramaswamy et al (2001), Radiative forcing of climate change, in: *Climate Change 2001: The*  
11 *Scientific Basis. Contribution of Working Group I to the Third Assessment Report of the*  
12 *Intergovernmental Panel on Climate Change*, Cambridge, UK: Cambridge University Press, 350-  
13 416.
- 14 Rivas-Martinez S. (1987), Mapa de las series de vegetacion de España. ICONA. MAPA. Madrid
- 15 Sagan, C., O.B. Toon and J.B. Pollack (1979), Anthropogenic albedo changes and the Earth's  
16 climate, *Science*, 206, 1363-1368.
- 17 Sanjuan, J.F. (2007), Deteccion de la superficie invernada en la provincia de Almeria a traves de  
18 imágenes Aster, Cuadrado-Gomez, I.M (ed.), Fundacion para la Investigacion Agraria de la  
19 Provincia de Almeria, Almeria.
- 20 Trenberth, K.E. et al. (2007), Observations: Surface and Atmospheric Climate Change. In: *Climate*  
21 *Change 2007: The Physical Science Basis. Contribution of Working Group I to the Fourth*  
22 *Assessment Report of the Intergovernmental Panel on Climate Change* [Solomon, S., D. Qin, M.

1 Manning, Z. Chen, M. Marquis, K.B. Averyt, M. Tignor and H.L. Miller (eds.)]. Cambridge Univ.  
2 Press, Cambridge, United Kingdom and New York, NY, USA.  
3  
4 Van Dam, O. (2000), Modelling incoming Potential Radiation on a land surface with PCRaster,  
5 POTRAD5.MOD manual. Utrecht: Utrecht Centre for Environment and Landscape dynamics,  
6 Utrecht University.  
7  
8 Vermote, E. F. and Vermeulen, A. (1999). Atmospheric correction algorithm: Spectral reflectances  
9 (MOD09), ATBD version 4.0.  
10  
11 Wang, X. L. (2003), Comments on “Detection of undocumented changepoints: A revision of the  
12 two-phase regression model,” *J. Clim.*, 16, 3383–3385.  
13  
14 Wigley, T.M.L., Ramaswamy, V., J.R. Christy and J.R. Lanzante (2006), Statistical issues  
15 regarding trends. In: *Temperature Trends in the Lower Atmosphere: Steps for Understanding and*  
16 *Reconciling Differences* [Thomas R. Karl, Susan J. Hassol, Christopher D. Miller, and William L.  
17 Murray, (eds)]. A Report by the Climate Change Science Program and the Subcommittee on  
18 Global Change Research, Washington, DC.

1   **CAPTIONS**

2

3   Figure 1. Study site. (a) SE Spanish INM Meteorological Stations used as temperature series  
4   controls: Murcia (MU), Granada (GR), Malaga (MA) and Almeria (AL) airports. Province of  
5   Almeria is shown in grey color. (b) Greenhouse farmland (GH) *Campo de Dalias* (in white).  
6   Agroclimatic Experimental Stations: Mojonera (MOJ) and Palmerillas (PAL).

7

8   Figure 2. Growth of land area dedicated to greenhouse farming from 1985 to 2007 in the study site  
9   (province of Almeria and coastal flatland *Campo de Dalias*) (Data from Sanjuan, J.F., 2007).

10

11   Figure 3. Annual mean surface air temperature anomalies time series for the six stations  
12   considered. A moving average of 2 terms has been applied to smooth the data. Anomalies are  
13   related to the reference period 1961-1990. MOJ and PAL related to AL average value.

14

15   Figure 4. Trends of the difference time series between stations for the period 1983-2006. Error bars  
16   showing 95% confidence intervals. \* Non significant ( $p>0.1$ ).

17

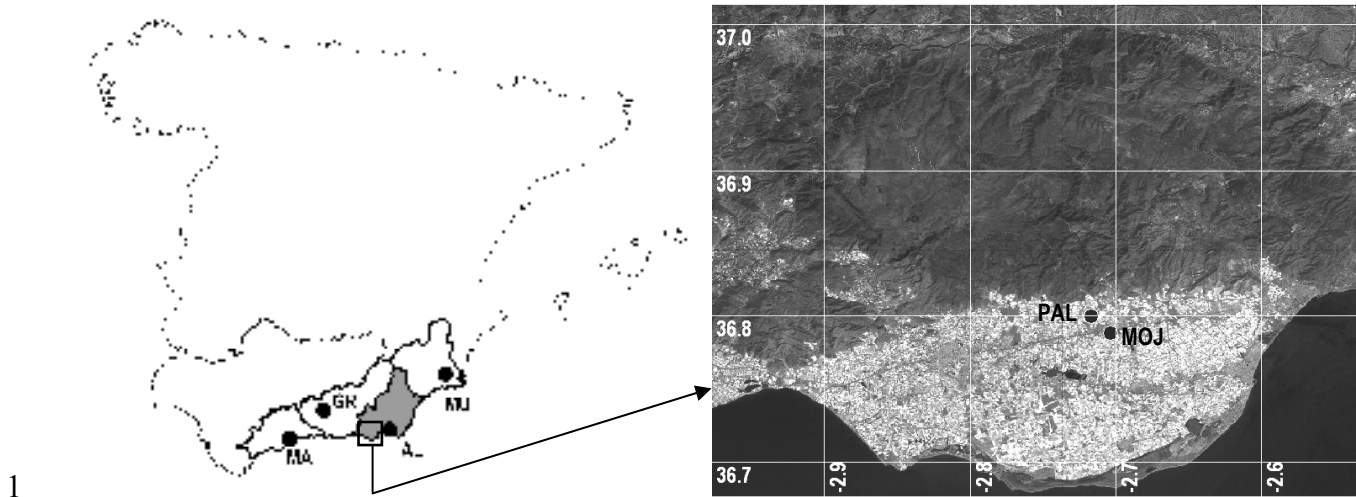
18   Figure 5. Seasonal variations of broadband albedos of greenhouse and pasture surfaces, and for the  
19   difference series (GH-P). Average values and for the period 2001-2005. The temporal variations  
20   (standard deviations) are plotted as vertical bars.

21

22   Figure 6. Seasonal variations of daily averaged outgoing shortwave radiation fluxes (OSR)  
23   reflected from greenhouse, pasture and the difference series (GH-P) between surfaces for the 2001-  
24   2005 period. The temporal variations (standard deviations) are plotted as vertical bars.

25

1 Table 1. Decadal trends and standard errors (in °C decade<sup>-1</sup>) of mean annual surface air  
2 temperatures for every meteorological station and for the periods 1972-2006 and 1983-2006. Trend  
3 values are estimated to be statistically significantly different from zero (at the 95% level).



1

2 a)

b)

3 Figure 1. Study site. (a) SE Spanish INM Meteorological Stations used as temperature series  
 4 controls: Murcia (MU), Granada (GR), Malaga (MA) and Almeria (AL) airports. Province of  
 5 Almeria is shown in grey color. (b) Greenhouse farmland (GH) *Campo de Dalias* (in white).  
 6 Agroclimatic Experimental Stations: Mojonera MOJ) and Palmerillas (PAL).

7

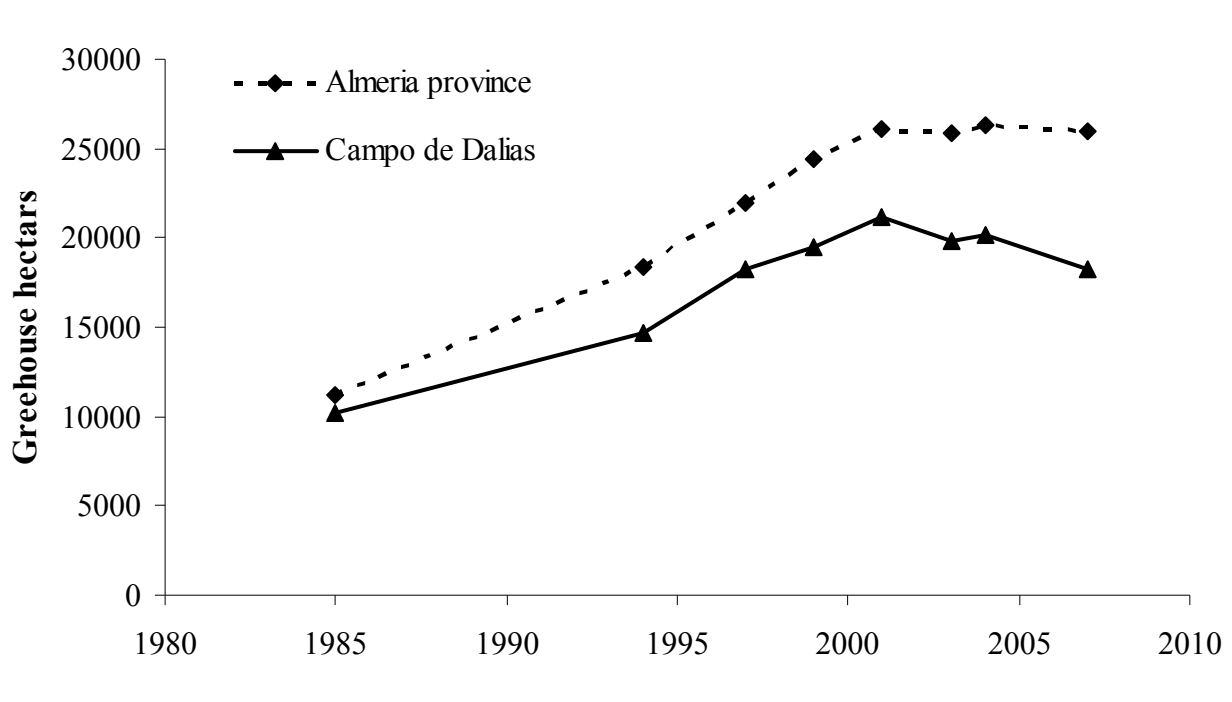
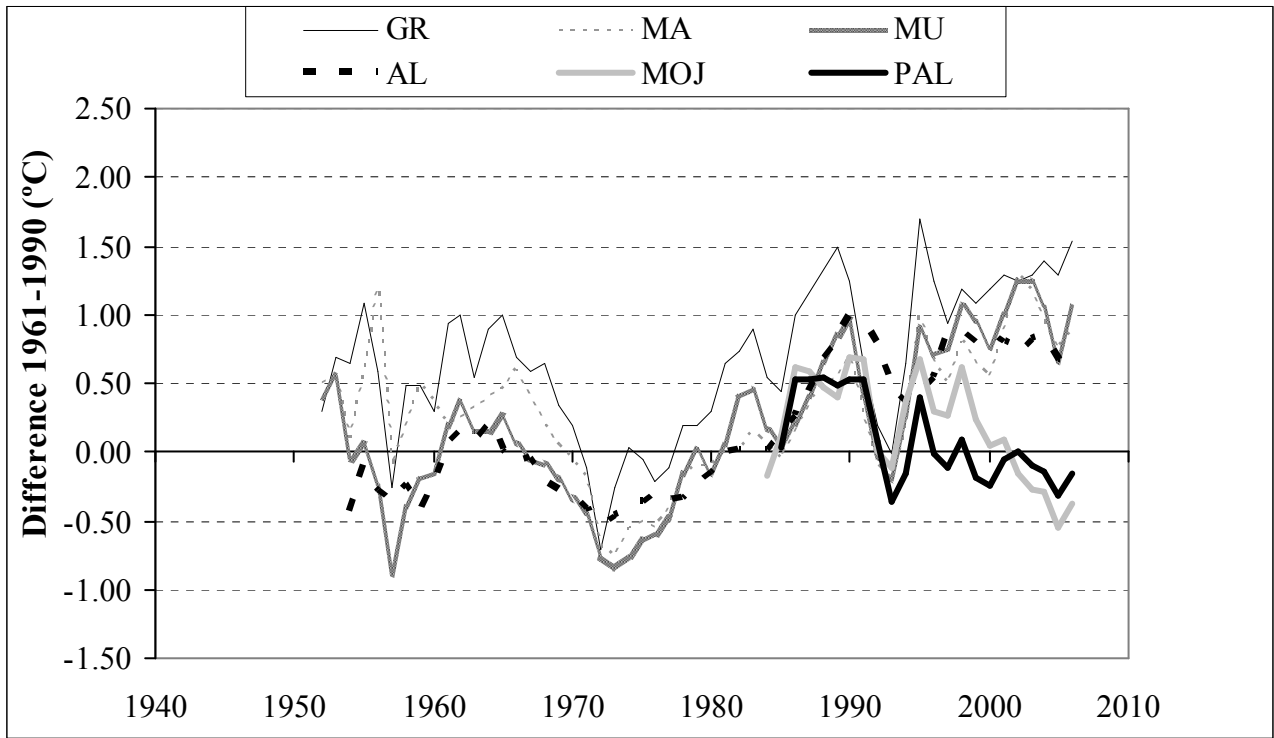


Figure 2. Growth of land area dedicated to greenhouse farming from 1985 to 2007 in the study site (province of Almeria and coastal flatland *Campo de Dalías*) (Data from Sanjuan, J.F., 2007).

1  
2  
3  
4  
5  
6  
7  
8  
9  
10  
11



12 Figure 3. Annual mean surface air temperature anomalies time series for the six stations  
13 considered. A moving average of 2 terms has been applied to smooth the data. Anomalies are  
14 related to the reference period 1961-1990. MOJ and PAL related to AL average value.

1  
2  
3  
4  
5  
6  
7  
8  
9  
10  
11  
12  
13  
14

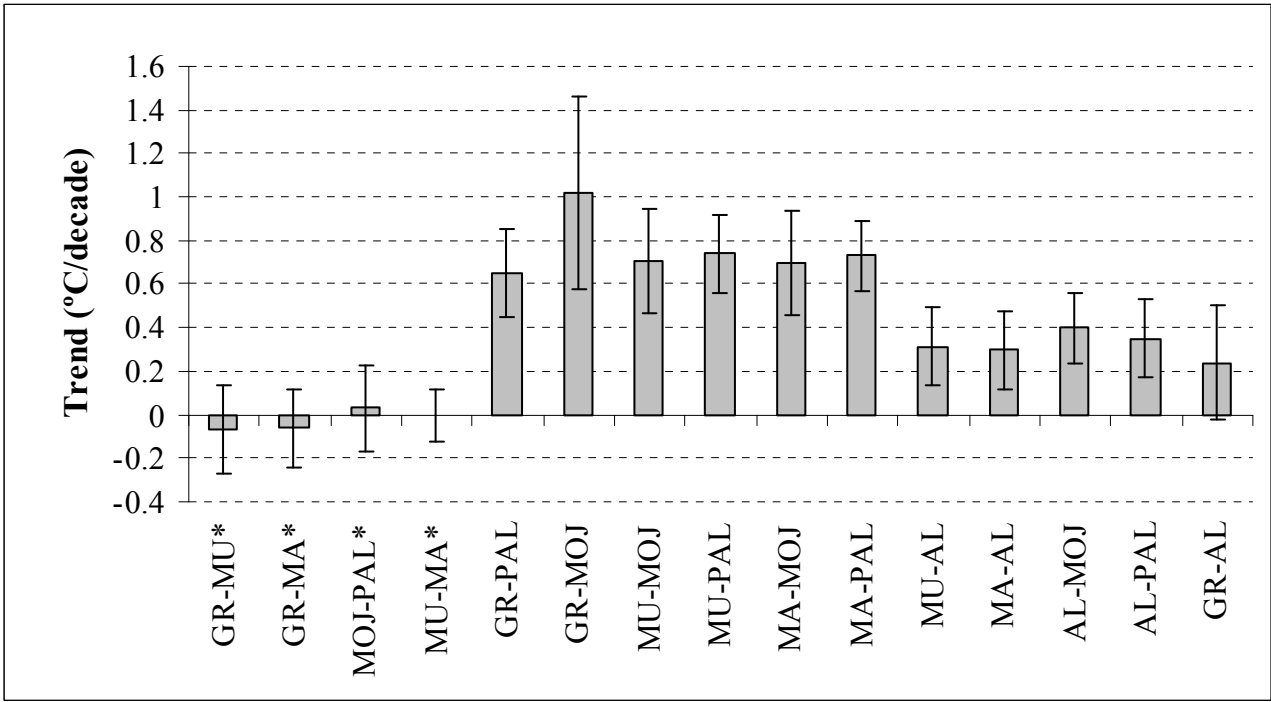
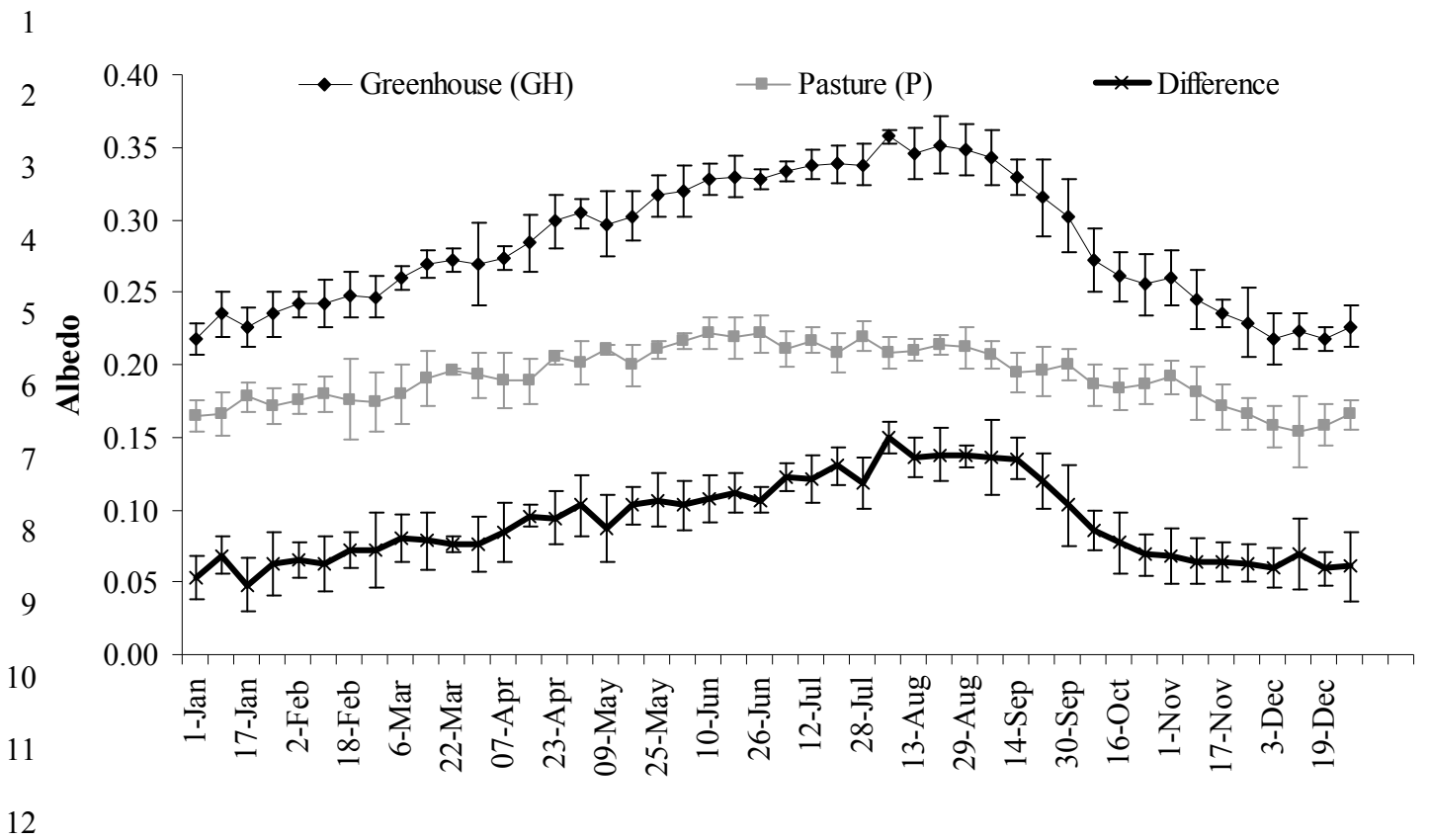
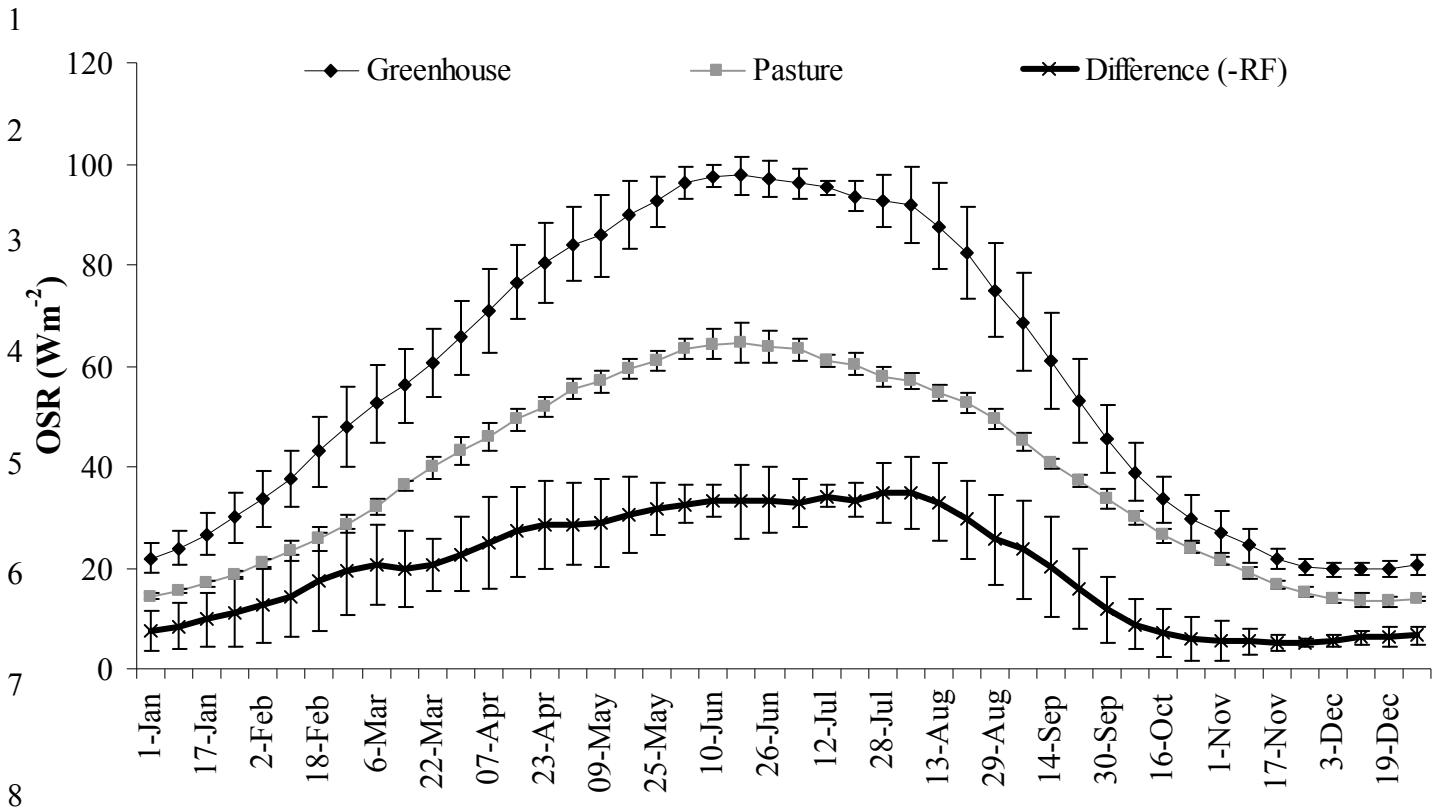


Figure 4. Trends of the difference time series between stations for the period 1983-2006. Error bars showing 95% confidence intervals. \* Non significant ( $p > 0.1$ ).



13 Figure 5. Seasonal variations of broadband albedos of greenhouse and pasture surfaces, and for the  
 14 difference series (GH-P). Average values and for the period 2001-2005. The temporal variations  
 15 (standard deviations) are plotted as vertical bars.



9 Figure 6. Seasonal variations of daily averaged outgoing shortwave radiation fluxes (OSR)  
 10 reflected from greenhouse, pasture and the difference series (GH-P) between surfaces for the 2001-  
 11 2005 period. The temporal variations (standard deviations) are plotted as vertical bars.

12

T <sup>a</sup> time series	MU	GR	MA	AL	MOJ	PAL
1972-2006	0.54 ± 0.07	0.48 ± 0.08	0.48 ± 0.06	0.37 ± 0.06	N/A <sup>b</sup>	N/A
1983-2006	0.43 ± 0.12	0.38 ± 0.17	0.40 ± 0.13	0.08 <sup>a</sup> ± 0.13	-0.29 ± 0.12	-0.32 ± 0.11

13 <sup>a</sup> Non significant at 95% level; <sup>b</sup> Non available data

14 Table 1. Decadal trends and standard errors (in °C decade<sup>-1</sup>) of mean annual surface air  
 15 temperatures for every meteorological station and for the periods 1972-2006 and 1983-2006. Trend  
 16 values are estimated to be statistically significantly different from zero (at the 95% level).

17